Desalination and Water Treatment
www.deswater.com
doi: 10.5004/dwt.2022.28667

267 (2022) 231–239
August

Batch, thermodynamic, and regeneration studies of Reactive Blue 19 using *Ulva reticulata* (biochar)

Venkat Saravanan Rajagopalan[a], Yuvaraja Rajendran[a], Andal Lakshumiah[a], Gokulan Ravindiran[b,*]

[a]*Department of Civil Engineering, Velammal College of Engineering and Technology, Madurai – 625 009, Tamil Nadu, India, emails: rvs2105@gmail.com (V.S. Rajagopalan), er.yuvaraja@gmail.com (Y. Rajendran), andalsureshkumar@yahoo.com (A. Lakshumiah)*
[b]*Department of Civil Engineering, GMR Institute of Technology, Srikakulam 532127, Andhra Pradesh, India, email: gokulravi4455@gmail.com/gokulan.r@gmrit.edu.in*

Received 25 April 2022; Accepted 2 July 2022

ABSTRACT

The goal of this study was to examine if *Ulva reticulata* biochar could be utilised in a batch approach to remove Reactive Blue 19 (RB19) from the liquid phase. To examine biochar features, the elemental analyzer, Brunauer–Emmett–Teller analyzer, proximate analysis, and Fourier transform infrared spectroscopy were utilised. As batch influencing factors, the sorbent quantity, solution pH, initial RB19 dye concentration, and temperature were all studied. Isotherm studies (Langmuir, Freundlich, Redlich–Peterson, and Sips), kinetic studies (pseudo-first-order and pseudo-second-order), and thermodynamic studies (Gibbs free energy, enthalpy, and entropy) were utilised to forecast the adsorption mechanism. Desorption studies were also conducted to determine the best elutants, solid-to-liquid ratios, and regeneration cycles to evaluate the performance of biochar in the sequential sorption and elution process.

Keywords: Reactive Blue 19; Biochar; Sorption; Isotherm; Thermodynamic

1. Introduction

Rapid urbanisation and population growth have resulted in increased water demand for both home and industrial reasons in recent years. Water is recognised as a vital resource for both human activity and industrial output. When compared to groundwater sources, surface water has been regarded as one of the most important sources of water in recent decades. However, in recent years, groundwater usage has expanded rapidly, resulting in groundwater depletion. Diary, dyeing, paper and pulp, paint, and brewing are some of the key industries that use a lot of water [1]. These industries rely heavily on surface freshwater for their operations. It is also anticipated that vast amounts of wastewater are created by these companies in the process of processing raw materials [2]. When this effluent enters the environment, it pollutes the water. As a result, hundreds of new harmful contaminants could enter the ecosystem via this effluent. When these harmful chemicals interact with surface water, they cause severe water contamination. These harmful chemicals are also making their way into the groundwater, causing groundwater pollution. A low concentration of harmful contaminants (less than 1 mg/L) will also have a bigger environmental impact. These dye molecules are not destroyed naturally and will remain in the water for an extended amount of time. Dye molecules are easily water-soluble, and removing these dye molecules has become one of the most difficult challenges in recent years. Dye molecules will serve as a thin barrier between the aquatic habitat and the surrounding environment. It fully prevents sunlight and dissolved oxygen from

* Corresponding author.

entering the atmosphere. This sunshine and dissolved oxygen are thought to be primary drivers of death for many aquatic species, and the river's self-purification capability has also diminished in recent years [3].

Many environmental protection authorities throughout the world have developed rules and standards for all businesses during the last decade. These organisations monitor and control pollution levels in the environment [4]. However, due to treatment efficiency, many counties continue to struggle to achieve this agency's standards. Water purification is the most challenging duty for the industry because it is incredibly expensive. Physical, chemical, and biological treatment methods are commonly classified into three types. Some of the most commonly used treatment techniques in businesses include sedimentation, coagulation, membrane filtration, electrocoagulation, and the filtering process [5]. However, developing pollutants cannot be removed using these procedures, and while membrane filtration is acceptable for all harmful pollutants, it is extremely expensive when compared to all other treatment methods. As a result, low-cost treatment is essential today [6]. Adsorption is a surface phenomenon involving the removal of adsorbate in the liquid or gas phase. Adsorption is one of the most widely used methods for removing hazardous substances in a variety of sectors. Natural clay, zeolites, hydrated silicates, and activated carbon are some of the most commonly utilised adsorbents. Because of its superior properties, activated carbon is the most extensively used adsorbent in the industry [7]. Many researchers have revealed that biosorption is one of the alternatives to the traditional adsorption technique [8]. Many adsorbents have been effectively synthesised from biomass, including leaf compost, agricultural waste, industrial sludge, natural seeds, fruit waste extracts, and seaweeds [9]. It has also been demonstrated that these adsorbents have the capacity to remove harmful contaminants from an aqueous solution.

Biochar, a carbon-rich substance, is created through gradual pyrolysis in the absence of oxygen. Biochar has multiple distinguishing features, including enhanced specific surface area, pore volume, pore radius, binding sites, and the presence of numerous functional groups. These properties will boost adsorption capacity toward harmful contaminants [10]. The current research looked on the production of biochar from the seaweed *Ulva reticulata*. *Ulva reticulata* is a member of the *Ulva* polysaccharide family and is high in carbonyl, carboxylic, alkyl, and amine groups. These functional groups will improve the adsorption capacity of the pollutants. Reactive dyes are one of the most commonly used dyes in the dyeing industry because to their various qualities. Water-resistant reactive dyes create a tight bond between the material and the colour. In the presence of aromatic rings, a strong covalent bond forms between the dye and the cellulose of the textile [11]. As a result, the focus of this investigation was on the elimination of Reactive Blue 19 using biochar made from *Ulva reticulata*.

2. Materials and methods

2.1. Seaweeds collection and chemicals

Ulva reticulata green marine seaweeds were obtained on the eastern coast of Tamil Nadu, India, near the Kanyakumari district. Along Tamil Nadu east coast, *Ulva reticulata* is frequently accessible in considerable quantities. Wet biomass was collected and rinsed three times with tap water before being washed with distilled water. These wet seaweeds were naturally dried in the sun for 24 h. Sun-dried biomass was shredded into 7.5 mm chunks and sieved to ensure uniformity. To guarantee that moisture was removed from the shredded biomass, it was placed in a hot air oven at 103°C for 25 h. Finally, the dried biomass was placed in a china crucible and firmly wrapped in thin aluminium foil with two holes cut in it. To determine the maximal biochar yield, the muffle furnace was operated at various temperatures ranging from 250°C to 400°C for 2 h. Finally, once the chain crucible reached room temperature, it was withdrawn from the muffle furnace and placed in a desiccator for further cooling [12].

2.2. Biochar characterization

The elemental analysis of the biochar was carried out using an elemental analyzer (2400 Series II-PerkinElmer). Proximate analysis was used to assess moisture content, ash content, fixed carbon content, and volatile matter content [12]. A Brunauer–Emmett–Teller (BET) analyzer is used to determine the specific surface area, pore radius, and pore volume of biochar. Functional groups in biochar, as well as pore size, pore volume, and specific surface area, play an important role in influencing the biochar's absorption ability during the adsorption process. The Fourier transform infrared spectroscopy method was utilised to search for functional groups in biochar (FT-IR). The samples were pretreated before FT-IR analysis.

2.3. Dye batch adsorption studies

The batch adsorption investigations were conducted using a temperature-controlled orbital shaker. Batch adsorption experiments were carried out in a 250 mL conical flask with a working volume of 100 mL. The requisite 1,000 mg/L stock solution was produced, and the desired concentration was obtained from it. To establish a continuous environment for the sorption process, the conical flask was filled with 100 mL of the required connection and the mouth of the conical flask was closed with cotton and sealed with aluminium foil over the cotton. The orbital shaker was operated at 160 rpm for 6 h. Following the completion of the equilibrium time, the sample was filtered and centrifuged to eliminate any suspended particulates in the solution. The transparent solution was used to measure the final concentration in a spectrophotometer after the centrifuge was run at 3,000 rpm for 10 min [12]. The dye molecule removal efficiency and charcoal sorption capacity were calculated using Eqs. (1) and (2).

$$Q = \frac{V\left(C_o - C_e\right)}{W} \tag{1}$$

$$\text{Removal efficiency} = \frac{\left(C_o - C_e\right)}{C_o} \times 100 \tag{2}$$

where Q is the sorption capacity (mg/g); V is the volume of the sample (L); C_o is the initial dye concentration (mg/L); C_e is the final dye concentration (mg/L); W is the mass of the biochar (g).

2.4. Modeling of isotherm and kinetics data

The Freundlich, Langmuir, Redlich–Peterson, and Sips adsorption isotherm models were fitted using the experimental data. The different isotherm models are represented by Eqs. (3)–(6).

Freundlich model: $$Q = K_F C_e^{1/n_F} \tag{3}$$

Langmuir model: $$Q = \frac{Q_{\max} b_L C_e}{1 + b_L C_e} \tag{4}$$

Redlich–Peterson model: $$Q = \frac{K_{\mathrm{RP}} C_{\mathrm{eq}}}{1 + a_{\mathrm{RP}} C_{\mathrm{eq}}^{\beta_{\mathrm{RP}}}} \tag{5}$$

Sips model: $$Q_e = \frac{K_S C_e^{\beta_s}}{1 + a_S C_e^{\beta_s}} \tag{6}$$

Adsorption kinetics is used to quantify absorption capacity over time at a constant concentration or pressure, resulting in a measurement of adsorbate diffusion into the pores of the biochar. Pseudo-first-order and pseudo-second-order kinetic models were used to fit the experimental data, as shown in Eqs. (7) and (8).

Pseudo-first-order model: $$Q_t = Q_e\left(1 - \exp\left(-k_1 t\right)\right) \tag{7}$$

Pseudo-second-order model: $$Q_t = \frac{Q_e^2 k_2 t}{1 + Q_e k_2 t} \tag{8}$$

2.5. Thermodynamic studies

The thermodynamic analysis was carried out to see if the Reactive Blue 19 (RB19) dye could be adsorbed onto charcoal (biochar). To investigate the adsorption process, the Gibbs free energy ($\Delta G°$), enthalpy ($\Delta H°$) and entropy ($\Delta S°$) were determined. The thermodynamic parameters were utilised to determine if the reactions were spontaneous or non-spontaneous, whether they were exothermic or endothermic, and the magnitude of the changes throughout the biochar surface [13]. The thermodynamic parameters were calculated using Eqs. (9) and (10).

$$\Delta G° = -RT \ln K_L \tag{9}$$

$$\Delta G° = \Delta H° - T\Delta S° \tag{10}$$

2.6. Elution and regeneration

The desorption efficiency of biochar is examined using spent biochar from the adsorption process. In a 100 mL conical flask, desorption experiments were carried out with a variety of elutants and solid-to-liquid ratios. The desorption tests were carried out for 120 min in a temperature-controlled orbital shaker with a rotating speed of 160. Sodium hydroxide, sodium carbonate, ammonium hydroxide, hydrochloric acid, methanol, and EDTA were among the chemicals studied. After the equilibrium contact time had expired, the sample was centrifuged for 5 min at 3,600 rpm. Before being analysed in a spectrophotometer, the supernatant was collected and filtered. The desorption efficiency was calculated by dividing the number of dye molecules in the solution after elution by the total amount of dye molecules accessible before elution. By changing the amount of the elutants, tests were carried out to optimise the number of elutants employed in the desorption process. The dye-free biochar is rinsed with distilled water before being exposed to 500 mg/L of Reactive Blue 19 for 120 min. Desorption was performed on this dye-bounded biochar once more. The purpose of the regeneration cycle experiments was to explore if biochar could be used to constantly sorb and elute colour molecules [14].

3. Results and discussion

3.1. Biochar characterization

Table 1 shows the basic properties of biochar at various temperatures. The results revealed a decrease in charcoal and an increase in pyrolysis. The carbon concentration of the biochar was one of the most important aspects of the sorbent. The carbon content decreased from 30.2% to 23.6% when the temperature was increased from 300°C to 500°C [15]. As the temperature rises, other components such as hydrogen, oxygen, nitrogen, and sulphur are also reduced. As a consequence, the optimal pyrolysis temperature for maximum biochar formation was determined to be 300°C. Proximate analysis determined the moisture content, ash content, volatile matter, and fixed carbon content to be 17.20%, 13.71%, 27.15%, and 41.94%, respectively. A BET analysis was carried out to better understand the surface characteristics of biochar. Raw and biochar had surface areas of 170.50 and 330.50 m^2/g, respectively, with pore volumes of 0.109 cm^3/g (raw) and 0.322 cm^3/g (biochar) and pore radius of 11.91 (raw) and 19.41 (biochar) and pore radius of 11.91 (raw) and 19.41 (biochar), respectively (biochar). Biochar contained more pores, and the availability of a greater specific surface area resulted in the most dye molecule sorption from the

Table 1
Elemental profile of biochar at varying pyrolysis temperature

Temperature (°C)	C (%)	H (%)	O (%)	N (%)	S (%)
300	60.2 ± 1.2	3.8 ± 0.2	25.9 ± 0.5	4.3 ± 0.2	5.8 ± 0.1
350	58.1 ± 1.2	3.4 ± 0.2	29.2 ± 0.5	4.2 ± 0.2	5.1 ± 0.1
400	56.6 ± 1.2	2.8 ± 0.2	32.3 ± 1.5	3.8 ± 0.2	4.5 ± 0.1
450	54.4 ± 1.2	2.5 ± 0.2	36.0 ± 1.5	3.4 ± 0.2	3.7 ± 0.1
500	53.6 ± 1.2	1.8 ± 0.2	38.9 ± 0.5	2.6 ± 0.2	3.1 ± 0.1

Mean ± SD

liquid phase [16]. Table 2 displays the FT-IR spectra of raw and dye-bounded biochar. The FT-IR results revealed that after the sorption process, there was a considerable shift in the spectra of different functional groups, which may be attributed to the dye molecules adhering to the various functional groups in the biochar. This may have been changed because the sulfonate groups in the dye molecules affected the functional groups on the biochar's surface [17].

3.2. Role of biochar dosage on RB19 adsorption

In the liquid and gas phases, the sorbent plays an important role in the sorption of harmful contaminants. With shifting properties, the sorbent must be more stable. The amount of sorbent used in the treatment process is proportional to the cost of treatment and the amount of secondary pollutants released into the environment. The fewer the adsorbents employed for sorption, the greater the benefits and the lower the treatment costs. The optimal sorbent dose and maximal removal of RB19 dye molecules were investigated in this work. The effect of biochar amount on RB19 dye sorption is shown in Fig. 1. According to the findings, an increase in biochar quantity enhanced the RB19 dye removal efficiency, resulting in decreased absorption capacity. The elimination effectiveness of RB19 was raised from 43% to 89% when the biochar quantity was increased from 1 to 10 g/L. Similarly, the biochar's sorption capacity was reduced from 215 to 44.5 mg/g. The sorbent's efficiency was determined by its removal efficiency and sorption capacity. Because the available sorbent pores and binding sites were very high and the dye concentration was insufficient for complete utilisation of the sorbent active sites, the removal efficiency was highest at the highest dosage [18]. As a result, a biochar dose of 2 g/L was determined to be optimal, with removal efficiency and absorption capacity of 81.8% and 204.5 mg/g, respectively.

Table 2
FT-IR spectra (before and after sorption)

Spectral groups	Raw biochar	RB19 dye bounded biochar
C–O (alcohol) band	1,111	1,132
Symmetric C=O	1,413	1,427
Asymmetric C=O stretch of COOH	1,611	1,648
C–H stretch	2,924	2,978
–NH, –OH stretching	3,457	3,466

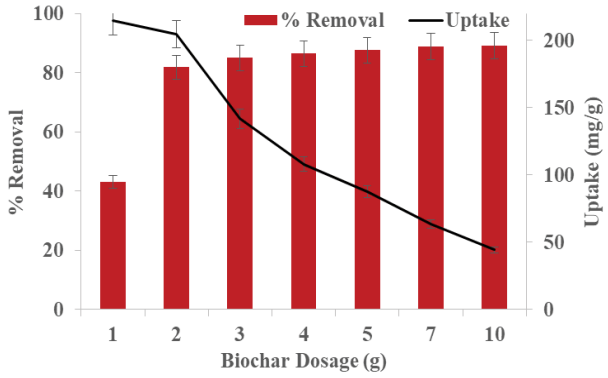

Fig. 1. Role of biochar concentration on RB19 removal using *Ulva reticulata*-derived biochar.

3.3. Role of equilibrium pH on RB19 adsorption

Negative ions are common in reactive dyes, and cellulose fibre is an electronegative ion as well [19]. The negative charges on the surface of the fibre are weakened by adding soda ash, which enhances the bonding nature of the reactive dyes and fibres. As a result, the wastewater generated by the dyeing process will be heavily polluted by alkaline nature. The concentration of negative ions will be extremely high. The extremely acidic region can be used to remove these reactive pigments from the wastewater. Because more protonated hydrogen ions are available in acidic circumstances, it is enriched with positive ions [20]. The positive and negative ions of reactive dyes will attract each other as a result. The pH of the water was varied from 2 to 5 in the current study. The effect of solution pH on reactive dye removal is depicted in Fig. 2. The data showed that increasing the pH reduced the efficacy of removal. It was discovered that when the pH was raised from 1.75 to 5, the removal efficiency reduced from 83.4% to 34%. Similarly, the uptake capacity was lowered from 208.5 to 85 mg/g. The optimum pH for eliminating reactive dyes was kept at 2 because there was little change in pH between 1.75 and 2.

3.4. Role of temperature on RB19 adsorption

In practise, the dyeing process will be carried out at a high temperature because this promotes dye-to-fabric adhesion. The temperature of the wastewater generated during the dyeing process will always be higher than that of the surrounding water bodies. The adsorption of dye molecules on the sorbent will also increase as the temperature rises. Fig. 3 depicts the influence of temperature on the removal of RB19 dye molecules. Increasing the temperature improved the removal efficiency, according to the data. The removal efficiency increased from 76.2% to 84% when the temperature was raised from 20°C to 45°C, for

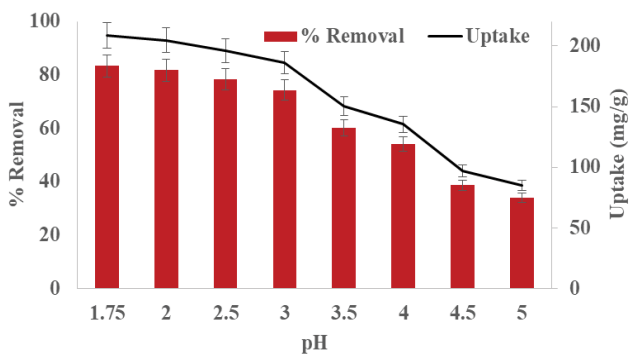

Fig. 2. Role of pH on RB19 removal using *Ulva reticulata*-derived biochar.

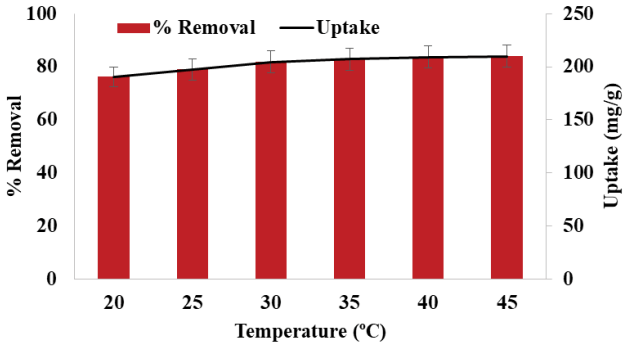

Fig. 3. Role of Temperature on RB19 removal using *Ulva reticulata*-derived biochar.

example. The sorption capacity was also increased from 190.5 to 210 mg/g. The higher elimination efficiency at high temperatures indicates that the process is endothermic. The results are compatible with thermodynamic research.

3.5. Isotherm and kinetics

Surface chemistry is one of the most important phenomena that deals with the interaction of adsorbate and adsorbent when they transition from the solid to the liquid phase. Adsorption isotherm models are one of the most effective tools for understanding surface chemistry. Physical adsorption or chemical adsorption can cause coloured molecules to adhere to the biochar. Between the adsorbate and the adsorbent, a weak van der walls force forms physical adsorption. Chemical adsorption, on the other hand, is defined by the formation of a strong chemical link between the adsorbate and the adsorbent [21]. The Langmuir, Freundlich, Redlich–Peterson, and Sips models are investigated in this work. The varied constants of each adsorption isotherm model are listed in Table 3. The monolayer adsorption capacity of biochar was expected to be 488.8 mg/g by Langmuir's model. The correlation coefficient between the anticipated and experimental uptakes was 0.9992, which is quite high and implies that monolayer adsorption occurred. The dye molecules were adsorbed in one layer over the sorbent, and the adsorbate molecules were bound by binding sites on the charcoal surface in the solid–liquid phase [22]. The Freundlich isotherm model investigates whether biochar is homogeneous or heterogeneous. The constant n_F represents the sorbent's heterogeneity in terms of magnitude. The value of n_F less than 1 (0.4885) suggests that the biochar's surface is heterogeneous. Furthermore, it demonstrates that adsorbate adsorption onto the surface of biochar is advantageous under all conditions. When compared to the Langmuir isotherm model, the correlation coefficient between experimental and projected uptake was 0.8383, which is lower. The Langmuir and Freundlich models are combined in the Redlich–Peterson isotherm model. The RP value of 0.98 implies that the equation will reduce to Langmuir and that the Langmuir adsorption isotherm will be the best fit for the current study. Similarly, the sorbent's dimensionless heterogeneity is explained using the Sips model.

Table 3
Adsorption isotherm model constants

Models		RB19
Langmuir	Q_{max}	488.88
	b_L	0.0079
	R^2	0.9992
Freundlich	K_F	18.177
	n_F	0.4885
	R^2	0.8383
Redlich–Peterson	K_{RP}	3.84
	α_{RP}	0.0023
	β_{RP}	0.98
	R^2	0.9986
Sips	K_S	1.1101
	β_S	1.4639
	a_S	0.0041
	R^2	0.9978

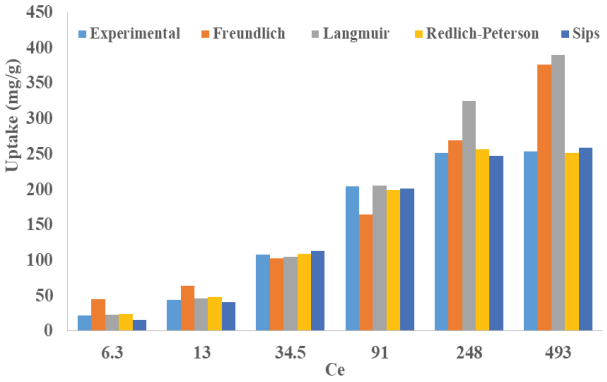

Fig. 4. Dye sorption isotherms on RB19 removal using *Ulva reticulata*-derived biochar.

Langmuir > Redlich–Peterson > Sips > Freundlich was the order of the isotherm models' correlation coefficients. As a result, the adsorption mechanism was determined to be based on the Langmuir isotherm model. Fig. 4 shows the anticipated absorption for various dye concentrations at the start.

Table 4 contains the kinetic model parameters. Adsorption kinetics is a method of determining the rate of reactions that may occur as a result of mass transfer, internal diffusion, or chemical reactions. The adsorption mechanism can be discussed in a step-by-step way as follows. External mass transfer between the adsorbent and the adsorbate; diffusion between a liquid phase and the adsorbent's outer surface; diffusion in adsorbent particles where the adsorbate enters the adsorbent's pores; formation of strong bonds between the adsorbent pores or binding sites and the adsorbate [23]. The uptake capacity predicted by pseudo-second-order models was superior to the pseudo-first-order kinetic model, as shown in Table 3, and it was over forecasted. For the pseudo-first-order kinetic model, the correlation coefficient (R^2) was

Table 4
Pseudo-first-order and pseudo-second-order kinetic model constants

Dyes	Model constants	Model constants	100 mg/L	250 mg/L	500 mg/L	750 mg/L	1,000 mg/L
Reactive Blue 19	Pseudo-first-order	Q_e	42.52	105.64	205.30	247.47	247.36
		k_1	0.0538	0.0471	0.0407	0.0405	0.0501
		R^2	0.9949	0.9978	0.9982	0.9963	0.9946
	Pseudo-second-order	Q_e	45.94	115.14	225.75	271.82	268.75
		k_2	0.0019	0.0006	0.0003	0.0002	0.0003
		R^2	0.9910	0.9905	0.9753	0.9900	0.9932

high. The experimental uptake was determined to be the best match for the pseudo-first-order kinetic models' anticipated update. The comparison of pseudo-first-order and pseudo-second-order kinetic models predicted and experimental data is shown in Figs. 5 and 6. The maximum sorption was achieved initially at 60 min, according to the kinetic analysis, and an increase in equilibrium time did not result in an increase in sorption capacity.

3.6. Thermodynamic studies

The thermodynamic parameters of the RB19 adsorption are presented in Table 5. Table 4 shows that at all temperatures, Gibbs' free energy is negative, indicating that the reactions are spontaneous. Because the Gibbs free energy increases with increasing temperature, this means that reactions are spontaneous at higher temperatures and non-spontaneous at lower temperatures [13]. Because the enthalpy and entropy values are both negative, the reaction is considered endothermic. Endothermic processes raise the system's entropy, and a positive enthalpy value implies that the reactions are endothermic. With a rise in temperature, endothermic processes will result in increased adsorption capacity. Enthalpy is also used to determine the type of sorption occurring between the adsorbate and the adsorbent. It implies physisorption and probable exothermic reactions if the heat evolved is between 2.1 and 20.9 kJ/mol. Whereas the heat released per mole is larger than 80 kJ/mol, chemisorption and endothermic processes are likely [13]. An enthalpy value of 73.84 kJ/mol was found in this investigation, which could imply a multi-sorption process. It's possible that the sorption was caused by physical or chemical adsorption. The presence of unpredictability in the solid–liquid phase, as shown by the positive value of entropy, could indicate structural changes in the adsorbate and adsorbent species. The mobility of adsorbate molecules/ions increases as the temperature rises, potentially boosting the adsorbate's affinity for the adsorbent [13]. Based on the Van't Hoff equation, Fig. 7 depicts the slope and intercept.

3.7. Reusability studies

Following sorption and elution of biochar, the sorption potential of a sorbent was investigated. Because the cost of producing biochar is so high, it is important to get the most out of it, therefore desorption tests were carried out. Because the amount of adsorbent required may be decreased, this technique will lower the overall cost of the adsorbent. The desorption efficiency of biochar was investigated using a

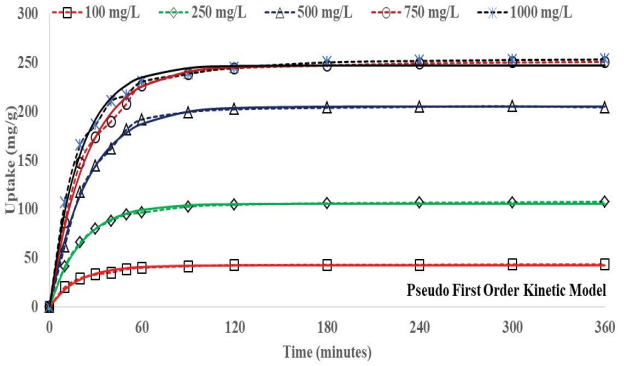

Fig. 5. Pseudo-first-order kinetic model observation on the removal of RB19.

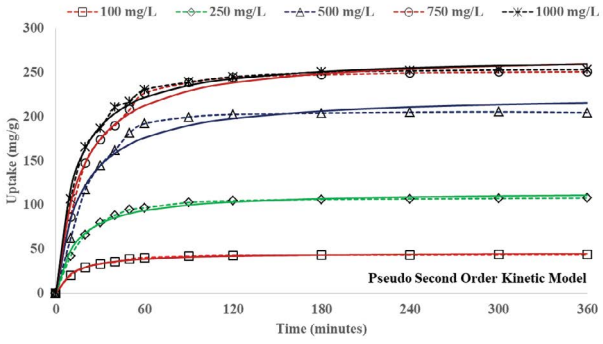

Fig. 6. Pseudo-second-order kinetic model observation on the removal of RB19.

Table 5
Thermodynamic parameters for the sorption of RB19

Dye	Temperature (K)	K_L (L/mol)	$\Delta G°$ (kJ/mol)	$\Delta H°$ (kJ/mol)	$\Delta S°$ (kJ/mol/K)
Reactive Blue 19	298	3.46	–3.08	73.84	0.20
	303	6.26	–4.62		
	308	14.80	–6.90		
	313	21.37	–7.97		
	318	28.23	–8.83		
	323	32.33	–9.34		

variety of elutants. According to the batch investigation, adsorption was greatest in the acidic area. As a result, it was obvious that desorption would be greatest in alkaline circumstances. The desorption efficiency of numerous elutants is depicted in Fig. 8. It is determined from Fig. 8 that alkaline elutants had a high desorption efficiency. Desorption efficiencies of sodium hydroxide, sodium carbonate, and ammonium hydroxide, for example, were 99.1%, 97.6%, and 89.2%, respectively. The desorption efficiency was also tested using the acidic elutant hydrochloric acid. The desorption efficiency of methanol and EDTA was very low and negligible. The best elutant for desorption of dye molecules from the sorbent was identified to be sodium hydroxide based on the results of the regeneration research.

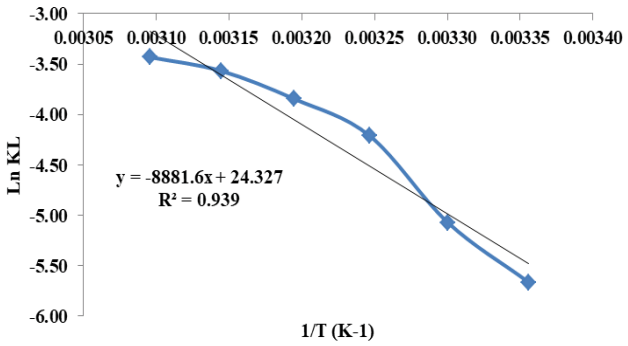

Fig. 7. Van't Hoff plot of RB19 onto *Ulva reticulata*-derived biochar.

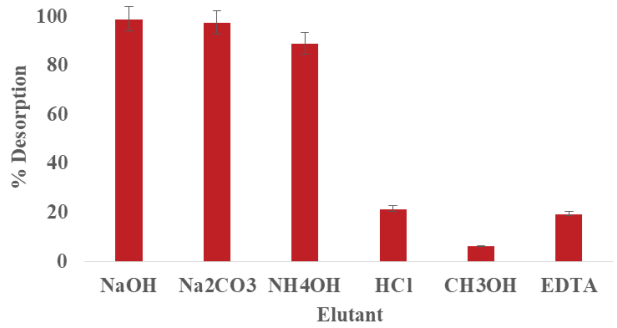

Fig. 8. Desorption efficiency of RB19 from biochar for different elutants.

The most efficient utilisation of elutant volume was researched further for the best elutant, sodium hydroxide. A separate treatment system may be necessary since the volume of elutants has such an impact on the cost of treatment and the emission of secondary pollutants. The sorbent of solute, also known as the solid to liquid ratio, is the volume of elutant necessary for maximum desorption of dye molecules attached to the charcoal. Fig. 9 displays the different S/L ratios. The S/L ratios of 1, 2, 3, and 4 resulted in desorption efficiencies of 99.1%, 99.1%, 99.1%, and 98.8%, respectively, according to the data. Desorption efficiency dropped by 94.1% when the S/L ratio was increased to 5. As a consequence, the optimal S/L ratio for maximal desorption efficiency was found to be 4. Fig. 10 depicts the biochar regeneration cycle. The biochar is evaluated for continuous sorption and elution for three cycles. For the regeneration cycles, a 0.1 M sodium hydroxide solution with a S/L ratio of 4 was utilised. The desorption efficiency of the first regeneration cycle was 99.1%, while the desorption efficiency of the third regeneration cycle was 99%. More than 95% desorption efficiency was routinely achieved. Table 6

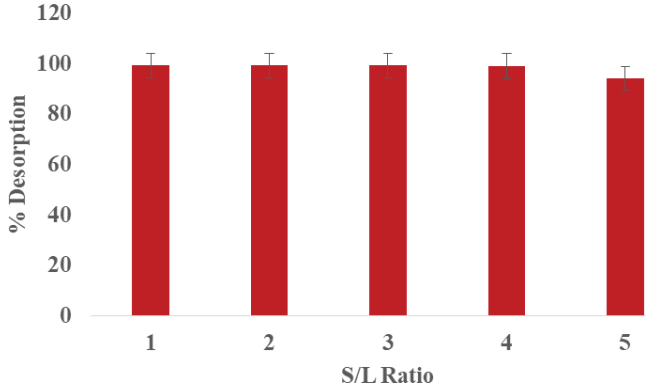

Fig. 9. Desorption efficiency of RB19 for varying solid to liquid ratio.

Table 6
Uptake capacity of Reactive Blue 19 using different sorbents

S. No	Adsorbent	Uptake capacity (mg/g)	References
1	Magnesium hydroxide modified biochar	103.09	[24]
2	CTS-TPP/MgO/Fe_3O_4 composite	120.3	[25]
3	Chitosan/MgO composite	512.82	[26]
4	Nanostructured magnesium oxide particles	250	[27]
5	Silica gel modified with 2,2′-(hexane-1,6-diylbis(oxy)) dibenzaldehyde	72.99	[28]
6	Grafted chitosan	1,498	[29]
7	Modified bentonite	123.50	[30]
8	Coconut shell derived biochar	96.95	[31]
9	Groundnut shell derived biochar	7.99	[32]
10	*Ulva reticulata* derived biochar	204.5	Present study

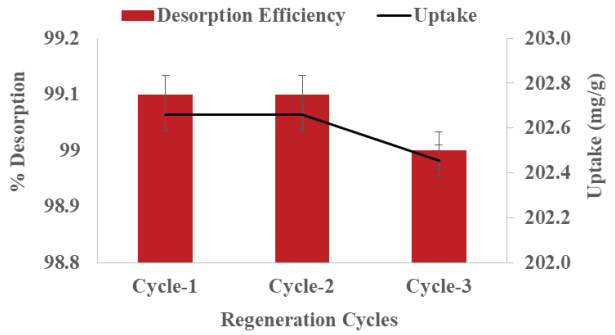

Fig. 10. Desorption efficiency of RB19 for varying regeneration cycles.

summarized different adsorbents used for the removal of Reactive Blue 19 from the aqueous solution.

4. Conclusion

The current work found that biochar made from *Ulva reticulata* can be utilised to successfully decolorize RB19 in a liquid phase. The removal efficiency was 81.8% and the absorption capacity was 204.5 mg/g at operating conditions of 2 g/L biochar, solution pH of 2, and temperature of 35°C. The Langmuir model was found to have the best fit, with a correlation coefficient of 0.9998. According to kinetic study, the pseudo-first-order kinetic model best fits the experimental data, with a correlation coefficient always more than 0.9946 for various concentrations. A thermodynamic analysis concluded that processes are endothermic and spontaneous under all conditions. Furthermore, a desorption study discovered that sodium hydroxide with a S/L ratio of 4 can be achieved, as well as three successive sorption and elution regeneration cycles.

Conflicts of interest

The authors declare that there is no conflict of interest.

References

[1] A. Abdolali, W.S. Guo, H.H. Ngo, S.S. Chen, N.C. Nguyen, K.L. Tung, Typical lignocellulosic wastes and by-products for biosorption process in water and wastewater treatment: a critical review, Bioresour. Technol., 160 (2014) 57–66.
[2] J. Kanagaraj, T. Senthilvelan, R.C. Panda, S. Kavitha, Eco-friendly waste management strategies for greener environment towards sustainable development in leather industry: a comprehensive review, J. Cleaner Prod., 89 (2015) 1–17.
[3] T. Robinson, G. McMullan, R. Marchant, P. Nigam, Remediation of dyes in textile effluent: a critical review on current treatment technologies with a proposed alternative, Bioresour. Technol., 77 (2001) 247–255.
[4] J. Rovira, J.L. Domingo, Human health risks due to exposure to inorganic and organic chemicals from textiles: a review, Environ. Res., 168 (2019) 62–69.
[5] E.A. Stefanescu, E. Soto-Cantu, Modern developments in the spray-drying industries, Recent Pat. Mater. Sci., 4 (2011) 106–121.
[6] S. Atalay, G. Ersoz, Green Chemistry for Dyes Removal from Waste Water: Research Trends and Applications, S.K Sharma, Ed., Wiley, 2015, pp. 83–117.
[7] M.O.A. Makinen, T. Jaaskelainen, J. Parkkinen, Improving optical properties of printing papers with dyes: a theoretical study, Nordic Pulp Pap. Res. J., 22 (2007) 236–243.
[8] M. Kucharska, J. Grabka, A review of chromatographic methods for determination of synthetic food dyes, Talanta, 80 (2010) 1045–1051.
[9] S. Kobylewski, M.F. Jacobson, Toxicology of food dyes, Int. J. Occup. Environ. Health, 18 (2012) 220–246.
[10] N.K. Lazaridis, T.D. Karapantsios, D. Georgantas, Kinetic analysis for the removal of a reactive dye from aqueous solution onto hydrotalcite by adsorption, Water Res., 37 (2003) 3023–3033.
[11] E. Mariani, C. Neuhoff, C. Villa, Application of high-performance liquid chromatography in the analysis of direct dyes in semi-permanent hair colouring cosmetics, Int. J. Cosmet. Sci., 19 (1997) 51–63.
[12] R. Gokulan, G. Ganesh Prabhu, J. Jegan, Remediation of complex remazol effluent using biochar derived from green seaweed biomass, Int. J. Phytorem., 21 (2019) 1179–1189.
[13] S. Papita, C. Shamik, T. Mizutani, Ed., Insight into adsorption thermodynamic, Chapter 16, Intechopen, 2011, pp. 349–364.
[14] R. Gokulan, J. Raja Murugadoss, J. Jegan, A. Avinash, Comparative desorption studies on remediation of remazol dyes using biochar (sorbent) derived from green marine seaweeds, ChemistrySelect, 4 (2019) 7437–7445.
[15] W.K. Kim, T. Shim, Y.S. Kim, S. Hyun, C. Ryu, Y.K. Park, J. Jung, Characterization of cadmium removal from aqueous solution by biochar produced from a giant *Miscanthus* at different pyrolytic temperatures, Bioresour. Technol., 138 (2013) 266–270.
[16] A.K. Priya, R. Gokulan, A. Vijay Kumar, S. Praveen, Biodecolorization of remazol dyes using biochar derived from *Ulva reticulata*: isotherm, kinetics, desorption and thermodynamic studies, Desal. Water Treat., 200 (2020) 286–295.
[17] I.M. Banat, P. Nigam, D. Singh, R. Marchant, Microbial decolorization of textile-dye containing effluents: a review, Bioresour. Technol., 58 (1996) 217–227.
[18] Z. Aksu, Ş.Ş. Çağatay, Investigation of biosorption of Gemazol Turquise Blue-G reactive dye by dried *Rhizopus arrhizus* in batch and continuous systems, Sep. Purif. Technol., 48 (2006) 24–35.
[19] K. Vijayaraghavan, Y.S. Yun, Competition of Reactive red 4, Reactive orange 16 and Basic blue 3 during biosorption of Reactive blue 4 by polysulfone-immobilized *Corynebacterium glutamicum*, J. Hazard. Mater., 153 (2008) 478–486.
[20] O. Gerçel, H.F. Gerçel, Adsorption of lead(II) ions from aqueous solutions by activated carbon prepared from biomass plant material of *Euphorbia rigida*, Chem. Eng. J., 132 (2007) 289–297.
[21] T.V.N. Padmesh, K. Vijayaraghavan, G. Sekaran, M. Velan, Application of two- and three-parameter isotherm models: biosorption of acid red 88 onto *Azolla microphylla*, Biorem. J., 10 (2006) 37–44.
[22] A.H. Jawad, A.S. Abdulhameed, A. Reghioua, Z.M. Yaseen, Zwitterion composite chitosan-epichlorohydrin/zeolite for adsorption of methylene blue and reactive red 120 dyes, Int. J. Biol. Macromol., 163 (2020) 756–765.
[23] J. Lehmann, S. Joseph, Biochar for Environmental Management: An Introduction, In: Biochar for Environmental Management: Science and Technology, 2012.
[24] W. Zhang, C. Du, N. Zhang, Z. Zheng, J. Tie, Reactive Blue 19 adsorption behaviors of magnesium hydroxide modified biochar derived from the traditional Chinese medical residual, J. Indian Chem. Soc., 99 (2022) 100517, doi: 10.1016/j.jics.2022.100517.
[25] A.H. Jawad, U.K. Sahu, N.A. Jani, Z.A. ALOthman, L.D. Wilson, Magnetic crosslinked chitosan-tripolyphosphate/MgO/Fe_3O_4 nanocomposite for Reactive Blue 19 dye removal: optimization using desirability function approach, Surf. Interfaces, 28 (2022) 101698, doi: 10.1016/j.surfin.2021.101698.
[26] N.K. Nga, N.T.T. Chau, P.H. Viet, Preparation and characterization of a chitosan/MgO composite for the effective removal of Reactive Blue 19 dye from aqueous solution, J. Sci.: Adv. Mater. Devices, 5 (2020) 65–72.
[27] N.K. Nga, P.T.T. Hong, T.D. Lam, T.Q. Huy, A facile synthesis of nanostructured magnesium oxide particles for enhanced

adsorption performance in Reactive Blue 19 removal, J. Colloid Interface Sci., 398 (2013) 210–216.
[28] A. Banaei, S. Samadi, S. Karimi, H. Vojoudi, E. Pourbasheer, A. Badiei, Synthesis of silica gel modified with 2,2′-(hexane-1,6-diylbis(oxy)) dibenzaldehyde as a new adsorbent for the removal of Reactive Yellow 84 and Reactive Blue 19 dyes from aqueous solutions: equilibrium and thermodynamic studies, Powder Technol., 319 (2017) 60–70.
[29] X. Jiang, Y. Sun, L. Liu, S. Wang, X. Tia, Adsorption of C.I. Reactive Blue 19 from aqueous solutions by porous particles of the grafted chitosan, Chem. Eng. J., 235 (2014) 151–157.
[30] Ö. Gök, A.S. Özcan, A. Özcan, Adsorption behavior of a textile dye of Reactive Blue 19 from aqueous solutions onto modified bentonite, Appl. Surf. Sci., 256 (2010) 5439–5443.
[31] R. Muralikrishnan, C. Jodhi, Biodecolorization of reactive dyes using biochar derived from coconut shell: batch, isotherm, kinetic and desorption studies, ChemistrySelect, 5 (2020) 7734–7742.
[32] R. Muralikrishnan, C. Jodhi, Biodecolorization of Reactive Blue 19 using biochar derived from groundnut shell: batch adsorption isotherms, kinetics and regeneration studies, Appl. Nanosci., (2022), doi: 10.1007/s13204-021-02212-9.